PROCEEDINGS, 49th Workshop on Geothermal Reservoir Engineering
Stanford University, Stanford, California, February 12-14, 2024
SGP-TR-227

Active Tracers for Hydraulic Control of Cooled Short Circuits: Bench-Scale Demonstration and Numerical Simulation

Adam J. Hawkins[1], Danni Tang[2], Aaron M. Baxter[1], Reeby Puthur[1], Daniel T. Korzukhin[1], Zach J. Zody[3], Bryan H. Abdulaziz[1], Patrick M. Fulton[3], Sarah Hormozi[1], Chris A. Alabi[1], Ulrich B. Wiesner[2] and Jefferson W. Tester[1]

Robert Fredrick Smith School of Chemical & Biomolecular Engineering[1], Materials Science & Engineering[2], Earth & Atmospheric Sciences[3], College of Engineering, Cornell University, 113 Ho Plaza, Ithaca, New York 14853, USA

ajh338@cornell.edu

Keywords: tracer, thermal-hydraulic performance, flow control

ABSTRACT

Commercially-successful geothermal systems require balance between thermal and hydraulic performance. An injector-producer well pair with exceptional hydraulic performance, for instance, may have inadequate thermal performance if the effective heat transfer surface area is insufficient. In such a circumstance the current state-of-the-art is to abandon such well pairs once production well temperatures fall below design/operating criteria. Here, an "active" tracer is introduced as a novel solution that enables cooled "short circuits" to be sealed off and circulating fluids to be redirected to hotter flow paths. This treatment increases the effective heat transfer area and subsequently improves thermal performance by increasing production well temperatures. Bench-scale laboratory experiments are presented and the anticipated improvement to thermal performance is determined from a hypothetical case.

1. INTRODUCTION

Hawkins et al. (2023) introduced a novel reservoir treatment method in which cooled short circuits can be eliminated and circulating fluids diverted to hotter flow paths. The treatment relies on circulation of an "active" tracer which selectively jams fluid flow paths below a pre-selected temperature threshold (i.e., the "lower critical solution temperature") (Figure 1). This temperature-responsive behavior is achieved via a microscopic hydrogel polymer that undergoes a counter-intuitive volume phase transition in which the polymer network collapses at high temperature and reversibly swells with water at low temperature. Here, progress towards synthesis of this "active" tracer is described and an updated forecast of thermal performance is given.

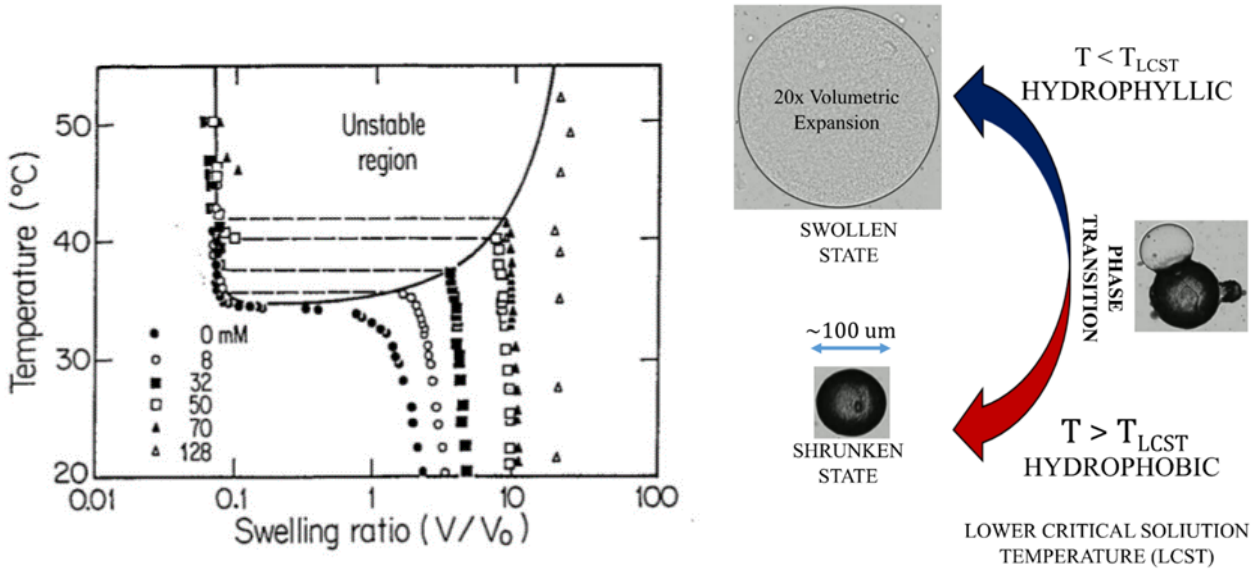

Figure 1: Phase diagram from Tanaka et al. (1985) (left) and schematic illustration of the reversible volume phase transition (right).

In the low-temperature, jammed state, the active tracer is designed to behave as a non-Newtonian fluid with a non-zero yield stress (i.e., a "yield-stress fluid"). In this state, the volume fraction (i.e., volume of "solids" divided by bulk volume) is above a critical point (Figure 2) (e.g., James et al., 2018). Therefore, the active tracer will jam inter-well regions if both local temperatures are below the lower critical solution temperature and if the local pressure drop is below the yield-stress. These two constraints offer two advantages: 1.) it prevents jamming close to the injection well where the strain rate is high and 2.) it prevents hot regions from jamming.

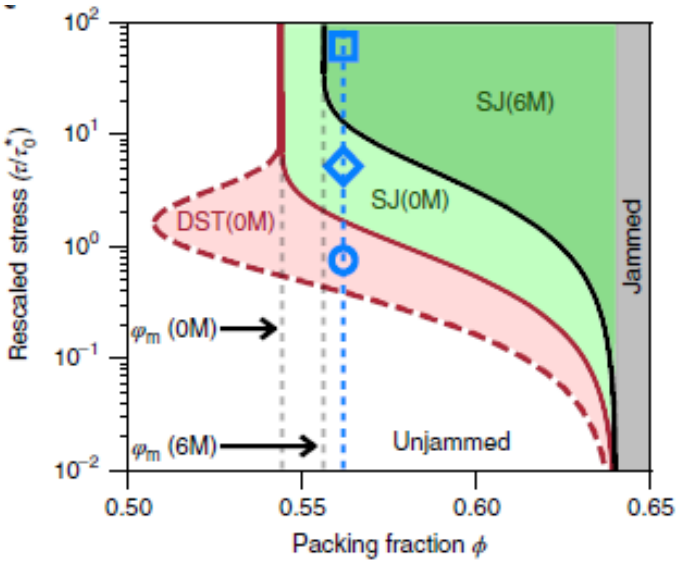

Figure 2: Shear jamming phase diagram from James et al. (2018). At packing fractions (i.e., volume fractions) larger than ~0.64 the system is in a jammed state. Below this value, the system is either in the unjammed state, a shear-jammed state (SJ), or in a discontinuous shear thinning state (DST). "0M" and "6M" correspond to the molarity of urea in solution, which is shown in the figure to alter the phase diagram.

2. ANTICIPATED IMPROVEMENTS

Here we consider a hypothetical circumstance modeled after the recent successes of Fervo Energy at Blue Mountain, Nevada (Fercho et al., 2023; Norbeck and Latimer, preprint). Three distinct scenarios are investigated, including: 1.) inlet-outlet short circuiting; 2.) ideal dipole flow; and 3.) improvements after treating the short-circuited case with the active tracer. To model inlet-outlet short circuiting, the fracture aperture distribution identified in Hawkins et al. (2020) is scaled up such that the inter-well spacing is roughly consistent with the two, long lateral wells at Blue Mountain (i.e., ~75 m well separation). We then simulate production well temperature drop from a single fracture over the course of 30 years with a mass flow rate of 3 kg/s and with an injection and initial temperature of 40 °C and 130 °C, respectively. Neglected transport phenomena are consistent with Hawkins et al. (2023), including temperature-independent viscosity, non-deformable fractures, and uniform fluid density (i.e., no buoyancy).

In the short-circuited state, these numerical simulations (solver first presented in Fox et al., 2015) forecast production well temperatures falling from its initial 130 °C to roughly 72 °C within 4 months of heat extraction (Figure 4). Such a circumstance is considered "premature thermal breakthrough" and presents substantial challenges to commercial success. Therefore, this non-ideal state is an ideal candidate to evaluate the improvements when the hydraulic control treatment is employed.

To simulate the effects of this improvement, we assume here that the lower critical solution temperature is 110 °C and that the material behaves as a yield-stress fluid when shear rates are below 100 Hz (Figure 3). First, the locations of the nodes of the finite element mesh that satisfy the two criteria for jamming are identified after a 7-day period of heat extraction. Then, the local aperture corresponding to these nodes is reduced by a factor of 30x to mimic the effect of the jammed state. Then, the simulation is reran with the post-treatment aperture and the subsequent improvements to thermal performance are plotted in comparison to the pre-treatment case and an ideal dipole flow scenario where the fracture aperture is uniformly 1 mm (Figure 4).

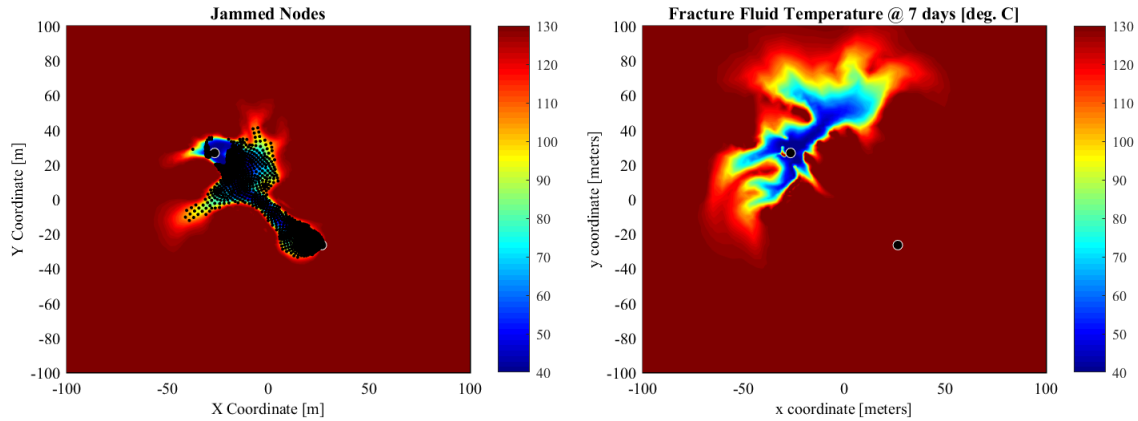

Figure 3: Fracture fluid temperature after 7 days of continuous cold water injection for the pre-treatment case (left) and the post-treatment case (right). The black dots on the left image correspond to the nodes of the finite element mesh that meet the two criteria for jamming.

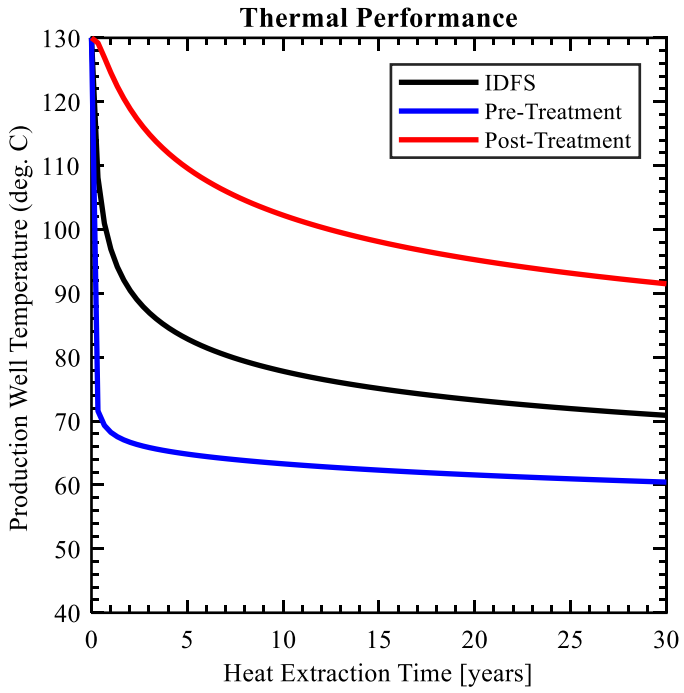

Figure 4: Production well thermal drawdown vs. time for the Ideal Dipole Flow Scenario (IDFS) (black line), the pre-treatment scenario (blue line), and the post-treatment scenario. (red line). The well separation and mass flow rate are 75 m and 3 kg/s, respectively and the initial injection and production well temperatures are 40 °C and 130 °C, respectively.

Based on these results, the active tracer treatment can significantly improve the thermal performance of the short-circuited case, even above the ideal dipole flow scenario (IDFS). Compare, for instance, the thermal power rating after 15 years for the three cases. The thermal power for the IDFS, the pre-treatment case, and the post-treatment case are 0.44 MW_{th}, 0.28 MW_{th}, and 0.74 MW_{th}, respectively.

3. SYNTHESIS UPDATE

Recent progress towards developing an ideal active tracer has focused on: 1.) developing the capability to tune the lower critical solution temperature; 2.) tuning the rheological properties; and 3.) scalability (Table 5). Tuning the transition temperature is achieved following the work of Tanaka et al. (1985) which showed that introducing ionic species elevates the transition temperature. Meanwhile, tuning the rheological properties is achieved by introducing an inorganic crosslinker along with an organic crosslinker. Details of these variations are described in a companion paper that will also be presented at the 49th Stanford Geothermal Workshop.

Table 5: Four distinct recipes with varying relative abundances of an inorganic clay crosslinker ("NC") and an organic crosslinker (OR) and the corresponding Lower Critical Solution Temperatures (LCSTs) and yield stresses. The three-dimensional swelling ratios vary broadly depending on solvents. The ranges reported here is for deionized water, synthetic groundwater, and synthetic ocean water.

SYNTHESIS ID	$NC_{X.X}$-$OR_{Y.Y}$	NIPA:SA	LCST	3D SWELLING RATIO	YIELD STRESS (Pa)
DTG-2017	$NC_{0.0}$-$OR_{1.2}$	90:10	105 °C	275x - 46,000x	70
DTG-2025	$NC_{2.0}$-$OR_{0.6}$	90:10	81 °C	723x – 3000x	45
DTG-2034	$NC_{0.0}$-$OR_{1.2}$	98:2	43 °C	836x – 23,219x	180
DTG-2043	$NC_{2.0}$-$OR_{0.6}$	98:2	43 °C	643x – 5000x	100

Here, this paper will focus on solvent-dependent behaviors, particularly solvent-dependent sizes and shrinking/swelling ratios. These properties were investigated using a flow-through microscope (Yokogawa Fluid Imaging Technologies, FlowCam 8000 series) equipped with a temperature-controlled inlet and temperature-controlled tubing (Figure 6). Four solvents were investigated, including deionized water, synthetic ground water, synthetic ocean water, and isopropyl alcohol. The results are given in Figure 7.

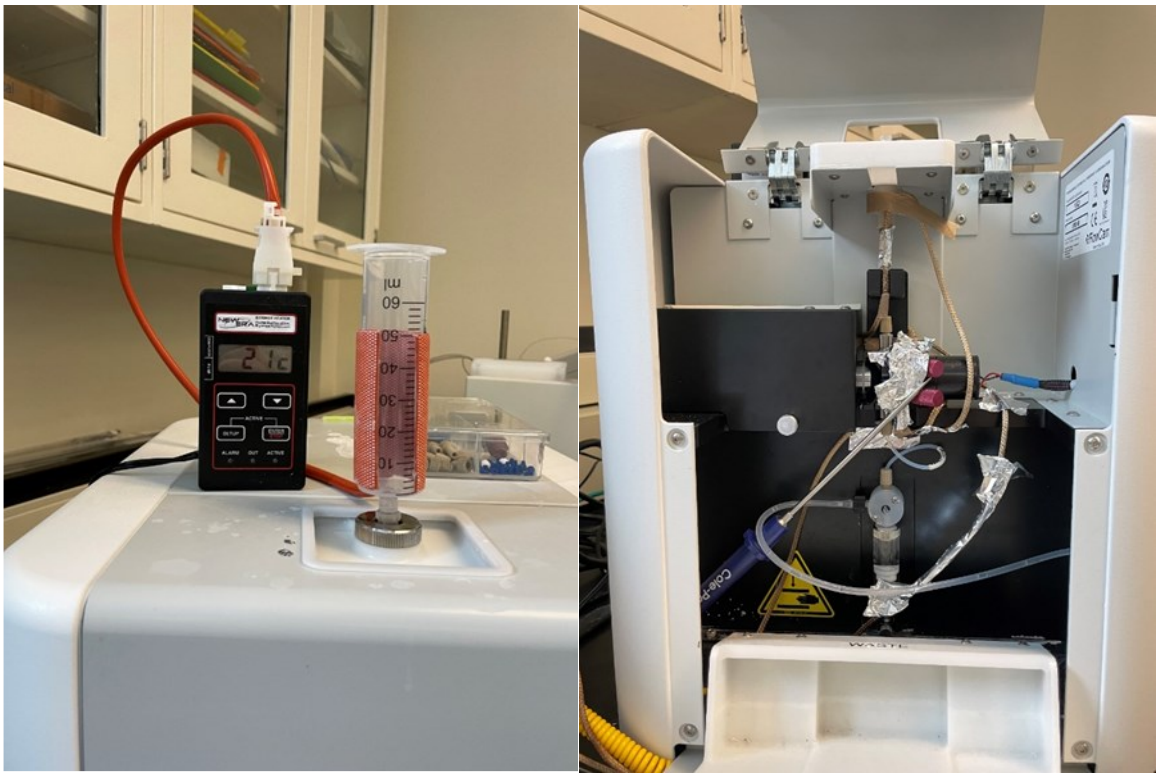

Figure 6: Temperature-controlled flow-through microscope (Yokogawa Fluid Imaging Technologies, FlowCam 8000 series).

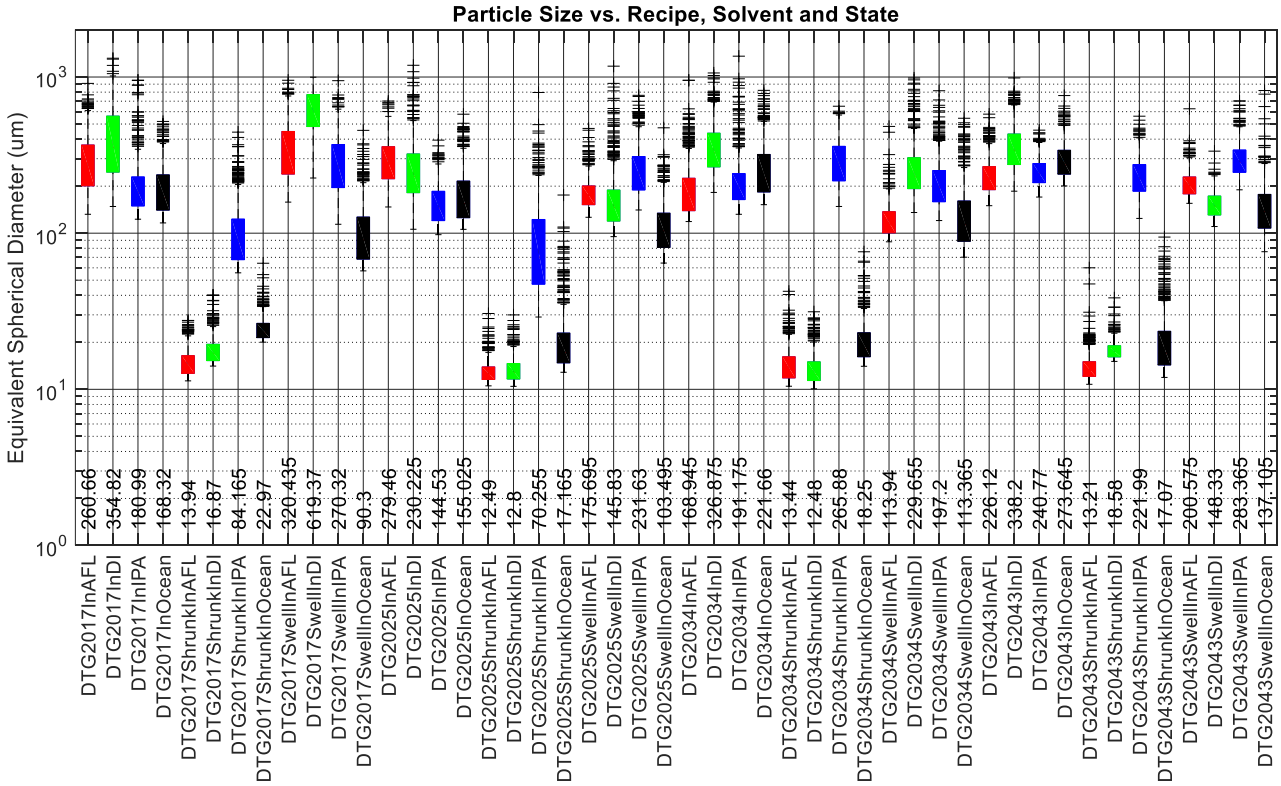

Figure 7: Box-and-whisker plot of particle sizes for four distinct recipes (DTG-2017, DTG_2025, DTG_2034, and DTG-2043) in varying solvents and states. The mean value is plotted as a dot and the number reported along the horizontal axis corresponds to the median particle diameter, as measured via the FlowCam apparatus.

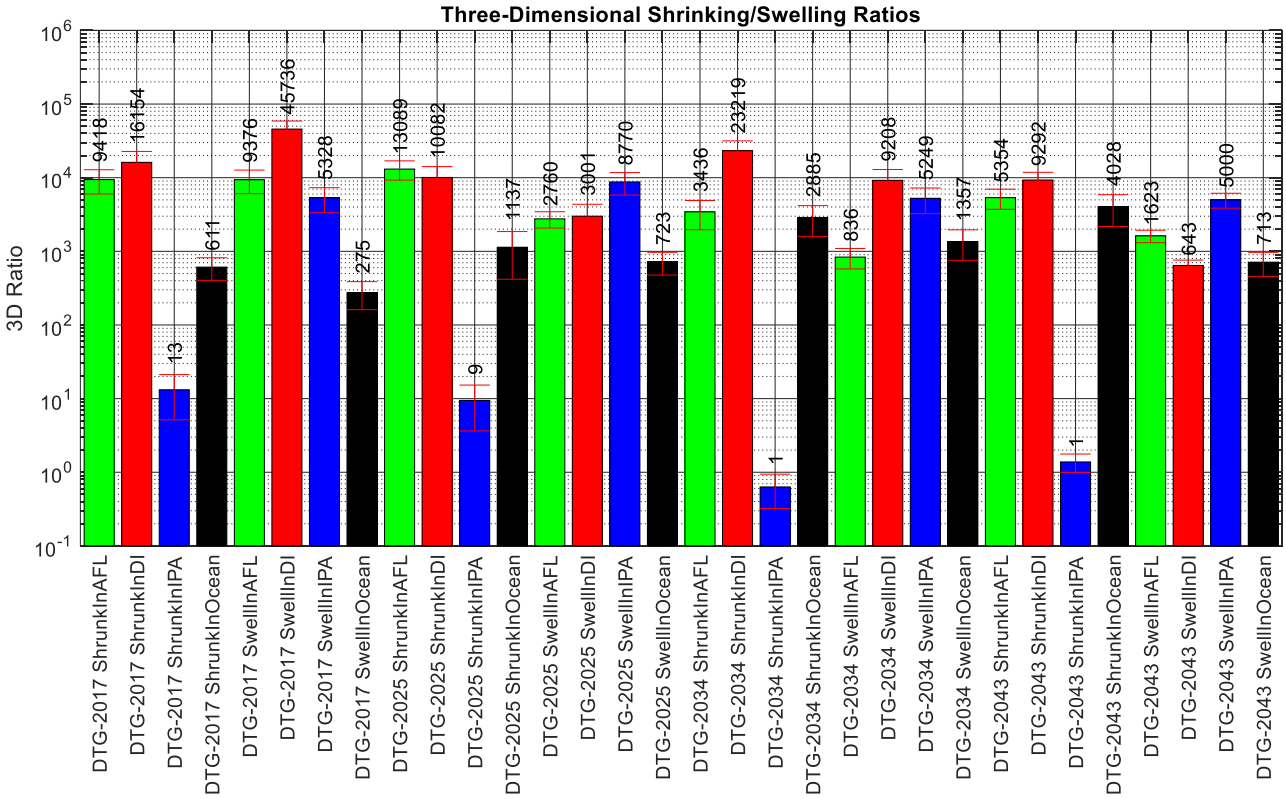

Figure 8: Three-dimensional swelling and shrinking ratios for four distinct recipes (DTG-2017, DTG-2025, DTG-2034, and DTG-2043) in varying solvents. Uncertainties are shown as red error bars and the value reported above the boxes corresponds to the mean of the shrinking and swelling ratios.

4. CONCLUDING REMARKS

This work presents a progress report on the development and testing of an active tracer for hydraulic control of cooled short circuits. This update investigated performance improvements for a hypothetical system and reports on solvent-dependent properties. Future work will continue to investigate the behavior of the active tracer in a bench-scale model system and at one or more larger, meso-scale field sites.

ACKNOWLEDGEMENTS

This material is based upon work supported by the U.S. Department of Energy's Office of Energy Efficiency and Renewable Energy (EERE) under the Geothermal Technologies Office, Award Number DE-EE0009786. The view expressed herein do not necessarily represent the view of the U.S. Department of Energy or the United States Government. Additional support provided by Cornell University College of Engineering.

REFERENCES

Fercho, S. et al.: Geology, State of Stress, and Heat in Place for a Horizontal Well Geothermal Development Project at Blue Mountain, Nevada, Proceedings, 48th Workshop on Geothermal Reservoir engineering, Stanford University, Stanford, CA (2023).

Fox, D. B. Koch, D. L. and Tester, J. W.: The Effect of Spatial Aperture Variations on the Thermal Performance of Discretely Fractured Geothermal Reservoirs, Geothermal Energy, 3, (2015).

Hawkins, A. J., Fox, D. B., Koch, D. L., Becker, M. W., and Tester, J. W.: Predictive Inverse Model for Advective Heat Transfer in a Short-Circuited Fracture: Dimensional Analysis, Machine Learning, and Field Demonstration, Water Resources Research, 56, (2020).

Hawkins et al.: Active Tracers for Hydraulic Control of Cooled Short Circuits, Proceedings, 48th Workshop on Geothermal Reservoir Engineering, Stanford University, Stanford, CA (2023).

James, N. M., Han, E., Lopez de la Cruz, R. A., Jureller, J., and Jaeger, H. M.: Interparticle Hydrogen Bonding can Elicit Shear Jamming in Dense Suspensions, Nature Materials, 17, (2018).

Norbeck, J. H., and Latimer, T. M.: Commercial-Scale Demonstration of a First-of-a-Kind Enhanced Geothermal System. *Preprint*.

Tanaka, T., Sato, E., Hirokawa, Y., Hirotsu, S., and Peetermans, J.: Critical Kinetics of Volume Phase Transitions of Gels, Physical Review Letters, 55, (1985).